Applying microCT and 3D Visualization to Jurassic Silicified Conifer Seed Cones: a Virtual Advantage Over Thin-Sectioning

Author: Gee, Carole T.

Source: Applications in Plant Sciences, 1(11)

Published By: Botanical Society of America

URL: https://doi.org/10.3732/apps.1300039

Applications in Plant Sciences

Applications in Plant Sciences 2013 1(11): 1300039

Application Article

Applying microCT and 3D visualization to Jurassic silicified conifer seed cones: A virtual advantage over thin-sectioning[1]

Carole T. Gee[2]

Steinmann Institute of Geology, Mineralogy, and Paleontology, Division of Paleontology, University of Bonn, Nussallee 8, 53115 Bonn, Germany

- *Premise of the study:* As an alternative to conventional thin-sectioning, which destroys fossil material, high-resolution X-ray computed tomography (also called microtomography or microCT) integrated with scientific visualization, three-dimensional (3D) image segmentation, size analysis, and computer animation is explored as a nondestructive method of imaging the internal anatomy of 150-million-year-old conifer seed cones from the Late Jurassic Morrison Formation, USA, and of recent and other fossil cones.
- *Methods:* MicroCT was carried out on cones using a General Electric phoenix v|tome|x s 240D, and resulting projections were processed with visualization software to produce image stacks of serial single sections for two-dimensional (2D) visualization, 3D segmented reconstructions with targeted structures in color, and computer animations.
- *Results:* If preserved in differing densities, microCT produced images of internal fossil tissues that showed important characters such as seed phyllotaxy or number of seeds per cone scale. Color segmentation of deeply embedded seeds highlighted the arrangement of seeds in spirals. MicroCT of recent cones was even more effective.
- *Conclusions:* This is the first paper on microCT integrated with 3D segmentation and computer animation applied to silicified seed cones, which resulted in excellent 2D serial sections and segmented 3D reconstructions, revealing features requisite to cone identification and understanding of strobilus construction.

Key words: *Araucaria*; Late Jurassic Morrison Formation; paleobotany; Pinaceae; phyllotaxy; three-dimensional image segmentation.

Although reproductive organs commonly hold the key to the taxonomy and phylogeny of plants, they are rare in the fossil record when compared to fossilized nonreproductive tissues such as shoots, wood, and leaves. The minute flowers and seeds that document the evolution of the earliest flowering plants, for example, are sometimes single lucky finds (Friis et al., 2011). Thus, when such a fortuitous discovery occurs, the decision to cut the specimen into sections to elucidate its internal construction is not an easy one to make, for traditional methods in paleobotany such as thin-sectioning or making polished longitudinal sections will cut into the rare reproductive organ. Serial thin-sectioning not only cuts up the entire fossil, but also destroys the parts of the fossil between the thin-sections. However, sectioning the fossil has been the only way to obtain essential information on the anatomy and internal construction of the plant.

[1]Manuscript received 14 May 2013; revision accepted 1 October 2013.

The author thanks P. Göddertz, G. Oleschinski, I. Ruf, and A. Schmitt for technical assistance; R. D. Dayvault, W. D. Tidwell, R. A. Stockey, R. Rössler, S. Flynn, M. Flynn, P. M. Sander, and M. Tsukagoshi for help in obtaining cones; and *APPS* Editor-in-Chief Theresa Culley, Lutz Kunzmann, and an anonymous reviewer for helpful comments. If not noted otherwise, photos and segmentations were made by the author. This is contribution no. 144 of the Deutsche Forschungsgemeinschaft Research Unit 533, "Biology of the Sauropod Dinosaurs," which generously provided travel funding.

[2]Email: cgee@uni-bonn.de

doi:10.3732/apps.1300039

In the Late Jurassic Morrison Formation, it has been hypothesized that the resident flora was species-poor and the vegetation sparse (Parrish et al., 2004) based on the lack of paleobotanical evidence. In fact, there is an abundance of permineralized wood in the Morrison Formation (Peterson, undated; Tidwell, 1990; Daniels and Dayvault, 2006; C. T. Gee, personal observation), much of which has not warranted further paleobotanical investigation because of a lack of internal preservation in the wood and perhaps also due to a paucity of Jurassic wood paleobotanists in North America. Moreover, even when fossil wood is well preserved anatomically, species diversity within a flora is difficult to determine based only on wood, as fossil wood commonly can only be determined to the family or genus level.

Hence, recent discoveries of reproductive organs such as silicified conifer seed cones in the Morrison Formation (Dayvault and Hatch, 2007) are lucky strikes that have tremendous potential to shed light on the diversity of the flora, especially given the diagnostic nature of megasporangiate strobili. Each fossil cone is thus precious, and the decision to prepare the fossil using a traditional technique such as thin-sectioning cannot be made without regret. The only two formally described species of conifer seed cone from the Morrison Formation known to date, *Hillistrobus axelrodii* Chandler and *Araucaria delevoryasii* Gee, are not silicified, but are preserved as carbonaceous compressions that do not offer any anatomical details (Chandler, 1966; Gee and Tidwell, 2010).

Fig. 1. Silicified conifer seed cones from the Late Morrison Formation in Utah, sorted into five cone morphotypes based on gross morphology and labeled by morphotype number. Each cone morphotype is exemplified here by one specimen, but in all morphotypes except for 3 and 4, there are several to many cones of each morphotype under study. All cones figured at the same relative size; scale bar = 1 cm. Cones 1, 5: Brigham Young University Museum of Paleontology Collection; cones 2, 4: Dayvault Collection; cone 3: Dinosaur National Monument collection. Photos by G. Oleschinski.

The recently discovered silicified conifer seed cones can be sorted into five new morphotaxa based on their comparative gross morphology and size (Fig. 1; Gee et al., in prep.). Yet basic information necessary for identification to the family level, such as the number of seeds per cone scale or the relative size and shape of the cone axis, is not usually evident from the exterior of the cone. Only in specimens of one cone morphotype, in which the distal part of the cone scale–bract complex are abraded to show the seed (cf. Dayvault and Hatch, 2007: figs. 17, 18), can the single-seeded nature in some cones be ascertained. There is thus an urgent need to look inside the cones.

This was the impetus for seeking and applying new methodology that would permit the sectioning of the cones without destroying them, otherwise known in paleontology as nondestructive sampling. Here I describe the application of high-resolution X-ray computed tomography—also called microtomography, or here, microCT—coupled with scientific visualization in the broadest sense to 150-million-year-old, silicified conifer seed cones from the Morrison Formation and to comparative material consisting of recent and other fossil conifer seed cones.

Although computed tomography is a tool that has been applied to paleobotanical problems for some years now (see, for example, Gee et al., 2003, who used a medical computed axial tomography [CAT] scanner to determine the size and amount of infilling of burrows and chambers in a rodent nut cache), the novelty of the present paper is the application of microCT integrated with two-dimensional (2D) visualization in the form of virtual single sections and serial sections, segmented three-dimensional (3D) reconstruction, size analysis, and computer animation to rock-hard, silicified conifer cones. The focus here is on the type of information that can be acquired on internal anatomy and construction using this integrated methodology. For example, image segmentation and 3D reconstruction are carried out on anatomical structures deeply embedded in plant tissue—in this case, seeds—to reveal seed phyllotaxy within fossil and recent conifer cones. The full botanical implications of the results produced by microCT and 3D visualization on the fossil and recent conifer cones, which are beyond the scope of this paper illustrating the application of a method and software within the context of a larger study, will be more fully addressed in subsequent work.

MATERIALS AND METHODS

The silicified cones come from the Late Jurassic Morrison Formation, and were discovered in the Brushy Basin Member, or at the boundary between the Brushy Basin Member and the underlying Salt Wash Member. The Brushy Basin Member is thought to have been deposited 150–145 million years ago (Kowallis et al., 1998). The silicified cones were found independently by private collectors at a number of localities in southeastern, eastern, and northeastern Utah (Fig. 2; see also Dayvault and Hatch, 2007, for detailed locality information) over the course of several decades, but have since been consolidated into two major collections: the Paleobotanical Collections of the Brigham Young University (BYU) Museum of Paleontology in Provo, Utah, USA, and the Dayvault Collection in Grand Junction, Colorado, USA.

Additional fossil cones from other Mesozoic sites were obtained for comparison from the Flynn Collection, Sheridan, Wyoming, USA; the Museum für Naturkunde Chemnitz, Chemnitz, Germany; and the Dana Quarry paleobotanical collection of the author.

To facilitate tracking specimens through the scanning and imaging process, individual cones that did not already bear an inventory number were assigned an inventory number with a CG prefix. To date, over 100 seed cones—48 fossil and 56 recent—have been scanned by microCT. This number is continually increasing as fossil and recent cones of particular interest are obtained.

The external morphology of the fossil cones was initially studied with a Wild M5 (Wild Heerbrugg, Heerbrugg, Switzerland) binocular microscope. Cones of each morphotype were then selected for microCT scanning based on their potential for internal preservation, although at least one cone of each morphotype was scanned. Furthermore, nearly all entire cones recovered from the Morrison Formation were scanned by microCT. Some fragmentary cones and a

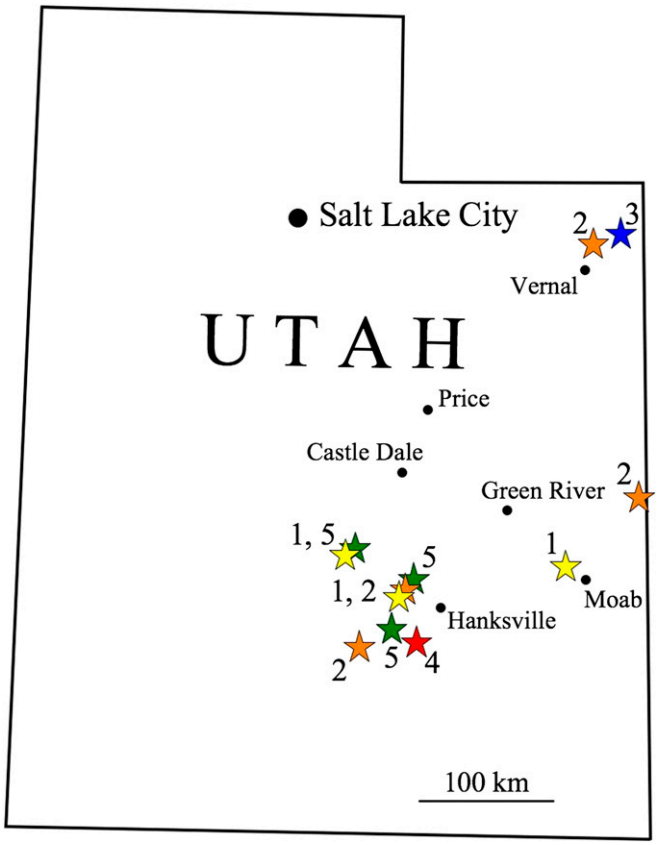

Fig. 2. Map of Utah marked with colored stars representing the localities at which the five cone morphotypes are found. The numbers correspond to the cone morphotypes in Fig. 1.

few longitudinally cut and polished cones were scanned as well to supplement the data set.

The microCT scanner used is a v|tome|x s 240D (phoenix|x-ray, General Electric Measurement & Control Solutions, Wunstorf, Germany), which is compact enough to be housed in a small basement room in the Division of Paleontology at the Steinmann Institute of Geology, Mineralogy, and Paleontology at the University of Bonn, Bonn, Germany. This microCT can scan specimens with the following maximum dimensions: 10 kg in weight, 420 mm in height, and 135 mm in diameter, which proved not to be limiting in the least for the fossil and recent conifer cones.

Without cutting, sawing, or inflicting any sort of damage, the cones were prepared by simply mounting each cone into a well-fitting styrofoam block that was especially carved out for its shape and size using a spoon. Alternatively, larger cones were placed in a custom-made mount made from a plastic bottle (Fig. 3). The cone and its nonmetallic mount were then firmly secured to the turntable stage of the microCT with adhesive materials such as packing or transparent tape. For the best resolution, the cone was aligned in a vertical position and carefully centered on the stage to enable the tube that generates the X-ray beam to get as close as possible to the specimen. Optimal centering of the cone on the turntable was determined using the preview function, which turned the cone and stage 360°; this made it possible to correct for any "wobble" of the cone's apex away from the rotational axis of the stage.

Maximum resolution—commonly defined as voxel size and measured on the micrometer scale—is dependent on the size of the specimen; the closer the specimen is to the microfocus tube that generates the X-ray, the better the resolution, the higher the magnification, and the smaller the voxel size. In elongate conifer cones, the limiting factor was height; in short and wide conifer cones, it was diameter. Because the conifer cones were of various heights and diameters, resolution was variable, ranging from 28 µm voxel size for the smallest cones to 135 µm for the most elongate cones. According to the manufacturer, the phoenix v|tome|x s 240D offers a maximum voxel resolution of less than 2 µm and detail detectability up to 1 µm (General Electric Measurement & Control, 2013).

The cones were then X-rayed with the microCT using the larger of the two tubes available: the 240 kV/320 W microfocus tube. Scan parameters such as kilovoltage (kV), current strength (µA), exposure time (ms), and number of projections (2D radiographs made longitudinally through the object) were variously set by the scan operator for each individual cone to obtain the best set of projections. The general rule is that higher voltage and current values are needed to produce a good range of gray values for dense material, such as found in silicified cones. A wide range in gray values in the density histogram will translate into good contrast and a good range of gray values in the final 2D images. The voltage and current values commonly used were in the range of 180 kV/180 µA to 200 kV/200 µA for silicified cones, compared to approximately 120 kV/120 µA for recent pinaceous cones and 150 kV/150 µA for recent araucariaceous cones. A third factor, exposure time (ms), can be used to boost image quality and to compensate for voltage or current to a certain extent.

A series of 600 to 1500 projections were made of the specimens. The number of projections is contingent on the maximum width of the cone in the scan area, based on a rule of thumb given by the manufacturer. The duration of scanning was between 20 and 60 min, although most cones were scanned for ca. 40 min.

The set of projections resulting from the scanning were processed with phoenix datos|x 2.0 (General Electric Measurement & Control Solutions), a CT software for fully automated data acquisition and volume processing. These data were then converted into 2D image stacks using the visualization and analysis software VG Studio Max (version 2.2; Volume Graphics, Heidelberg, Germany), which is integrated with the phoenix datos|x 2.0 software and came as a package with the phoenix v|tome|x s scanner. The result was a virtual series of sections through the specimens in the transverse plane (x-y), as well as in two longitudinal planes (x-z, y-z). These image stacks could be saved in various formats, including as TIFF and JPEG files.

Single sections, or orthoslices, from these image stacks could then be opened and studied using an application such as Preview 5.5.1 (719.11) developed for Mac OS X (Apple, Cupertino, California, USA). Alternatively, the images were studied as a continuous series of serial sections using VG Studio Max (Volume Graphics GmbH, Heidelberg, Germany) or the biological visualization software Fiji (ImageJ 1.47), which is freely available on the Internet (http://fiji.sc/; Schindelin et al., 2012); both of these applications provide a window viewer on which the sections can be quickly flipped through using the scroll wheel on the computer mouse or the slider bar under the window.

Although VG Studio Max can be used for three-dimensional reconstruction, or volume rendering, the three-dimensional imaging of structures within the cones was carried out in this study with the visualization and analysis software Avizo (version 7.1; FEI Visualization Sciences Group, Düsseldorf, Germany), because of its superior segmentation capabilities in which internal structures are "segmented," that is, selected on the basis of their gray values, then depicted in color in a 3D reconstruction. In the case of the fossil conifer cones, these internal structures were primarily the seeds, vascular system, or cone scales. When a tissue consists of discrete elements, such as the continuous row, or spiral, of seeds in some conifer cones that extend from the cone base to the cone apex, the discrete elements can be segmented in the same color to show their association to one another. For example, in the segmentation of seed spirals in the current study, a light green for the row of seeds that began lowest (most proximally) in the cone was consistently used, then an orange and a light blue for the next two rows of seeds, respectively, to facilitate comparison between different individual cone specimens and between morphotypes.

Quantitative measurements of internal structures, such as the length or width of the seeds, were also made using Avizo. Computer animations, or videos, of 2D transverse and longitudinal serial sections through a *Pinus pinea* L. cone were produced using the software virtualdub (version 1.9.10), which is freely available on the Internet (http://www.virtualdub.org/). The computer animation of the segmented 3D reconstruction of the same cone, on the other hand, was created using Avizo.

RESULTS

The projections produced by microCT are digital X-ray images. As in medical X-rays, the densest tissues are depicted by the lightest colors, whereas the tissues lightest in density show up as the darkest colors. When the series of projections made by the microCT of a cone are converted into image stacks, a series of virtual sections are produced that are equivalent to 2D sections in serial sections produced by thin-sectioning.

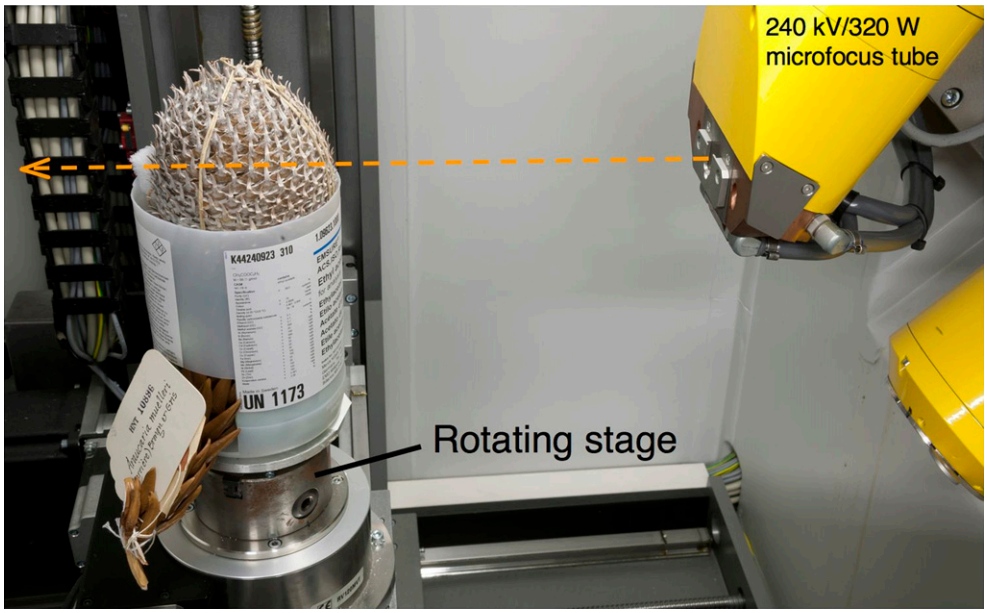

Fig. 3. Example of a recent seed cone of *Araucaria muelleri* (Carrière) Brongn. & Gris being scanned by microCT. The conifer cone is secured upright in a custom-made, nonmetallic mount that is fastened to the turntable stage with double-sided tape. Right, the electronic tube, from which the X-ray beam (arrow) is generated and shot through the cone. This cone, on loan from the Huntington Botanical Gardens Herbarium, San Marino, California, USA, is not part of the data set discussed in the paper. Photo by G. Oleschinski.

These virtual sections are, however, initially monochrome, ranging from white to multiple shades of gray to black, unlike actual thin-sections or polished longitudinal sections, which may show internal structures that have been colored differentially by diagenetic processes. The distance between microCT sections, called slices, is also very small; the finest spacing in this conifer cone study was 28 µm in a narrow fossil cone (CG061). In comparison, in thin-sections, even when the properties of the embedding rock matrix are ideal, the minimum thickness between sections is at least 4 mm (O. Dülfer, University of Bonn, personal communication). Most importantly, microCT does not damage or alter the specimen in the least, and sections of the cones in the three planes (transverse and the two longitudinal planes) are obtained without specimen loss due to

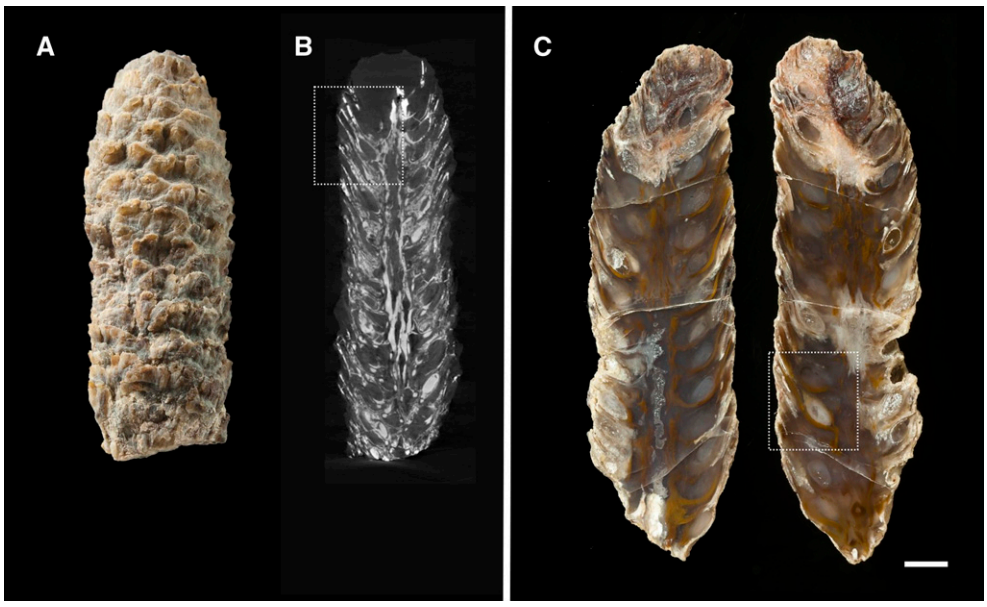

Fig. 4. Two cones of morphotype 2 figured at the same relative size; scale bar = 5 mm; both from the Dayvault Collection. (A) Lateral surface view of cone taken by conventional photography (specimen no. CG016). (B) The same cone as in Fig. 1 (cone 2), but shown in a longitudinal X-ray section produced by microCT. Boxed area is shown enlarged in Fig. 5A. (C) Another cone of morphotype 2 that was prepared using the traditional method of cutting and polishing in longitudinal section, and imaged using conventional photography (specimen no. CG017a, b). Boxed area is shown enlarged in Fig. 5B. Photos A and C by G. Oleschinski.

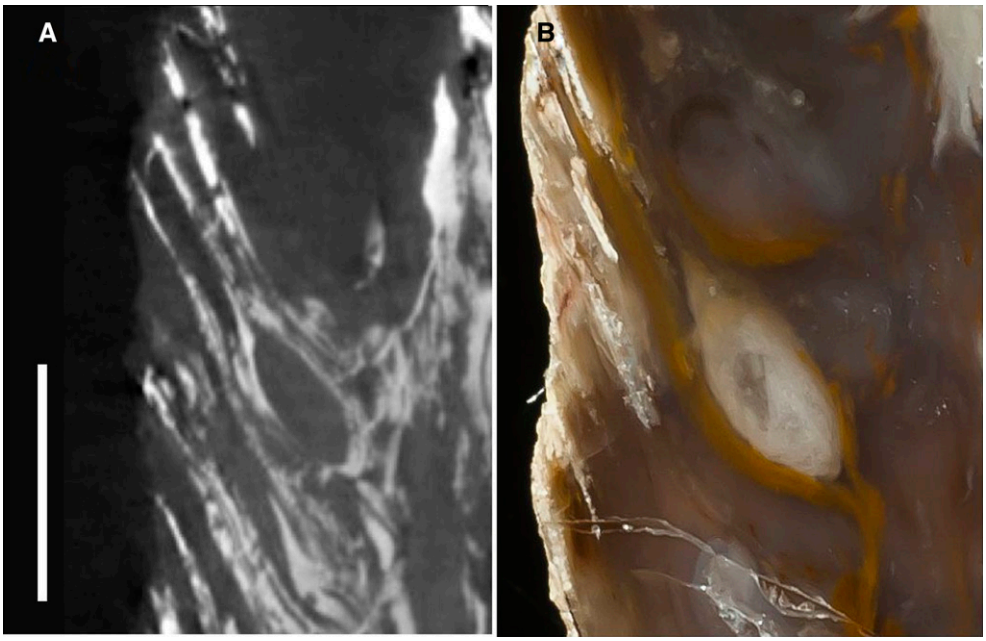

Fig. 5. Detail of a seed-bearing cone scale from two different cones of morphotype 2 to compare fidelity of imaging; scale bar = 5 mm. (A) MicroCT; boxed area from Fig. 4B. (B) Conventional polished longitudinal section; boxed area from Fig. 4C. Photo B by G. Oleschinski.

sawing, grinding, or reorientation of the specimen for cutting in another plane of section, as is the case with traditional thin-sectioning.

The fossil cones of the same morphotype found at the same locality in the Morrison Formation tended to have the same quality of preservation and imaging results. Thus, it was generally found that among the five cone morphotypes, two display clear internal structure (Fig. 1, cones 2 and 5), two show indistinct traces of internal structure (Fig. 1, cones 1 and 3), and one is obviously a natural cast in which only the external surface of the cone is preserved (Fig. 1, cone 4).

Fidelity of structures in the microCT images—The cone morphotype showing the best set of internal details is cone morphotype 2 (Fig. 1, cone 2; Figs. 4, 5), in which the seeds, cone scales, cone axis, and vascular system are visible in the digital images (Figs. 4B, 5A). A comparison of two cones of morphotype 2—an intact cone scanned by microCT (Fig. 4A, B) and a second specimen that was cut and polished in longitudinal section (Fig. 4C)—reveals that the microCT image faithfully portrays the internal details of the intact cone. This is especially apparent in the angle of attachment of the cone scales to the cone axis, the length and thinness of the cone scale, the size and shape of the ovule, and the position of the ovule at the base of the scale (Fig. 5A, B). The one major feature absent in the microCT image is the information resulting from the color differentiation of tissues that is evident in the polished section. However, adding artificial color to selected parts, known as *image segmentation* or simply *segmentation*, can more clearly delineate internal structures or tissues from one another; the application of segmentation is discussed below.

The internal tissues or structures of some silicified cones could not be clearly observed with microCT, which was the case with cone morphotype 1. In this instance, this was surprising because spectacular natural coloration of internal tissues in the cones, which is due to differing amounts of mineral trace elements, could be observed in a polished longitudinal section (e.g., Fig. 1, cone 1). Furthermore, in the case of a three-dimensionally preserved cone from contemporaneous sediments in Wyoming that was preserved as a carbonaceous fossil (Fig. 6)—that is, not silicified—no internal structure is evident using microCT. In

Fig. 6. Conventional photography of a conifer seed cone from the Morrison Formation of north-central Wyoming that is preserved as a 3D, carbonaceous fossil (not silicified); scale bar = 1 cm; from the Dana Quarry paleobotany collection of the author. Unlike the silicified cones, the microCT of this carbonaceous cone did not show any internal detail. Photo by G. Oleschinski.

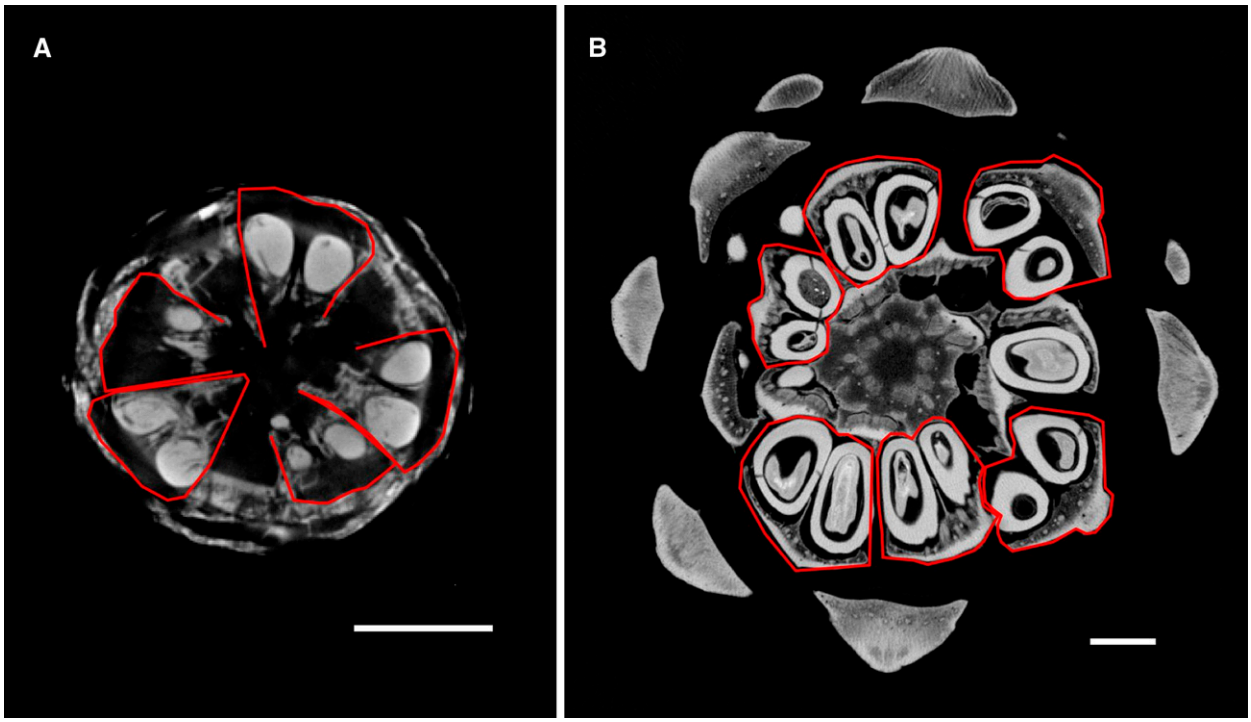

Fig. 7. Transverse sections produced by microCT showing two seeds per cone scale (red lines added postscan), which is characteristic of the Pinaceae; scale bars = 1 cm. (A) Morphotype 2 cone (specimen no. CG061, transverse section 198/945; Dayvault Collection). (B) Recent *Pinus pinea* (transverse section 448/875).

both of these cases, the microCT images are completely black and featureless.

***2D sections and serial sections*—**Determining the number of seeds borne by each cone scale or cone scale–bract complex is of utmost importance for the determination of a cone to the family level. In the cones in which some internal anatomical structure can be observed with microCT, this character appears quite clearly in transverse section. In a fossil cone of morphotype 2, for example, there are clearly two seeds per cone scale (Fig. 7A). For comparison, a recent cone of *Pinus pinea*, the Italian stone pine, which also bears two seeds per scale–bract complex, is also illustrated (Fig. 7B).

An interesting and potentially useful taxonomic character for differentiating between some conifer families that appeared in the course of this study is the phyllotaxy of the cone scales and seeds. The phyllotaxy of plant parts in living plants is well known as a basic character for identification, and there has been some work on applying leaf phyllotaxy in fossil conifers to distinguish species from one another (e.g., Harris, 1976; Watson et al., 1987).

When examining a pine cone such as *P. pinea*, it is quite clear that the cone scales, and therefore the seeds, are arranged in a spiral, from the base to the apex of the cone (Fig. 8A). What is less obvious, however, is how many seed spirals are found within a cone, the number of times each seed spiral wraps around a cone, and the number of seeds in the 360° revolution of a seed spiral. It is unclear, even when looking down at the apex or up at the base of a cone, whether the cone scales are arranged in a clockwise or counterclockwise fashion (Fig. 8B; see also Rutishauser and Peisl, 2001).

Determining how many seed spirals are found within a cone and whether the spirals turn in a clockwise or counterclockwise fashion (chirality) is also best observed in transverse section, as opposed to radial or tangential section, when viewing 2D sections. In transverse sections of the *P. pinea* cone produced by microCT, there are clearly three spirals of seeds arranged in a clockwise fashion (Fig. 8C). In a cone that is as short and wide as *P. pinea* (Fig. 8A), the triad of seed spirals and their chirality are not evident in every transverse section. Rather, the transverse sections must be studied serially, by moving up and down

→

Fig. 8 (see p. 7). Spiral phyllotaxy of cone scales and seeds in Pinaceae and putative pinaceous cones. The direction and number of the seed spirals are highlighted, respectively, by red arrows or segmentation of individual spirals; all scale bars = 1 cm. (A–D) A recent cone of *Pinus pinea*, showing a spiral arrangement of cone scales. In lateral (A) and distal (B) view, it is unclear from viewing the exterior of the cone how many spirals there are and in which direction they turn. Only in transverse section (C; transverse section 448/875) or as a three-dimensional reconstruction (D) do the three, clockwise spirals of seeds become apparent. (E–I) Three fossil cones of morphotype 2, each with three seed spirals; all from the Dayvault Collection. In this species, seed spirals can be arranged in a clockwise (E, F) or counterclockwise (G–I) direction within individual cones. (E, F) Specimen no. CG016 in transverse section (E; transverse section 464/1001) and as a three-dimensional reconstruction (F) in which the seed spirals and vascular system (yellow) are segmented. This is the same specimen as in Figs. 4A, 4B, and 5A. Note the clockwise arrangement of the seed spirals. (G, H) Specimen no. CG061 in transverse section (G; transverse section 198/945) and as a three-dimensional reconstruction (H) in which only the seeds are segmented. In this case, the seed spirals run in a counterclockwise fashion. (I) Specimen no. CG064, reconstructed in three dimensions, and again showing three spirals of seeds that run counterclockwise. Photos A and B by G. Oleschinski; segmentation of D, F, H, I by A. Schmitt.

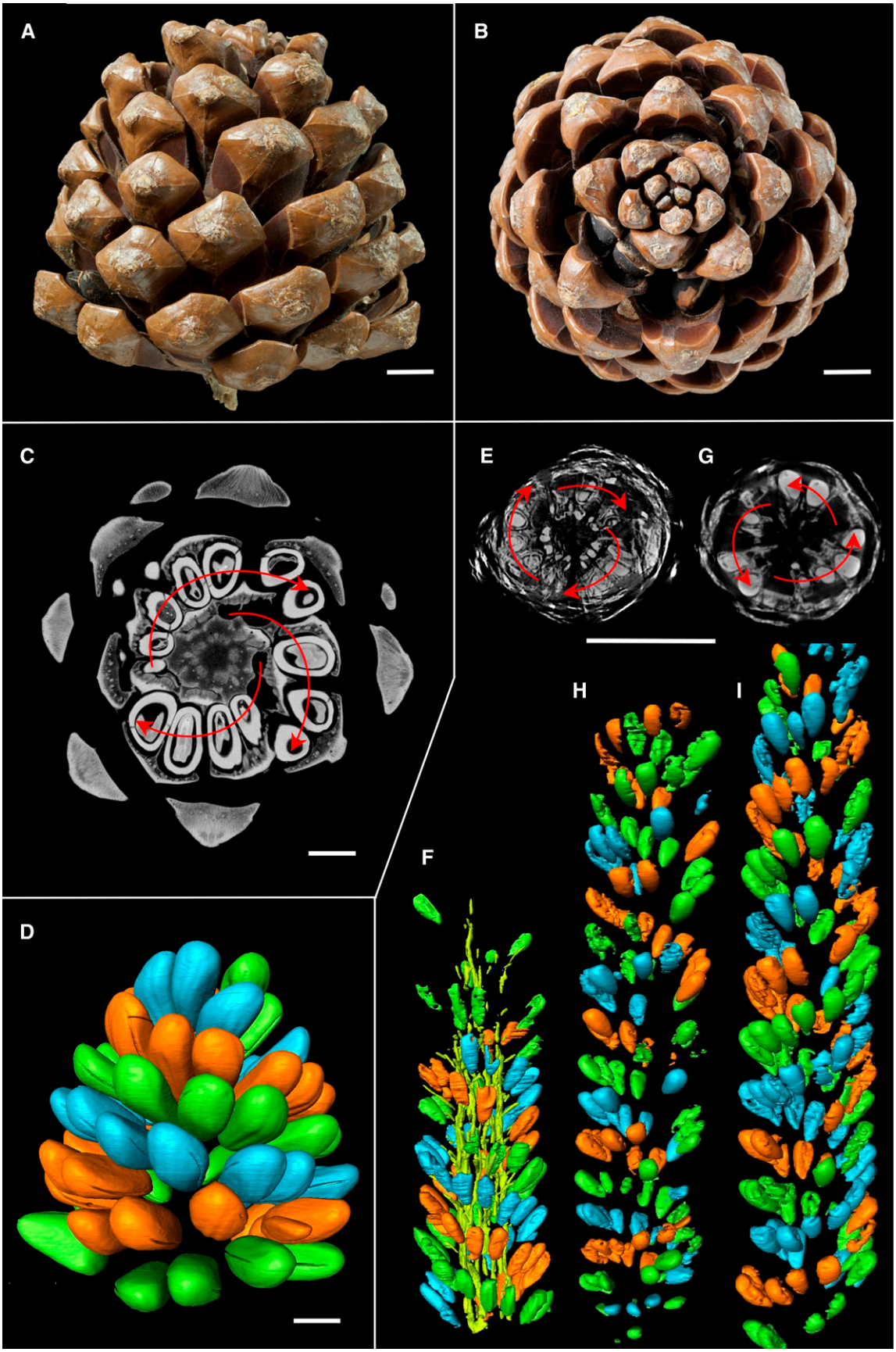

through the cone, section by section, to find the right view that will show the three seed spirals and their directionality. In the *P. pinea* cone under study, this appears about midway through the cone. This becomes clearly evident in the computer animation of the serial transverse sections through the *P. pinea* cone, in which the three clockwise seed spirals appear at roughly 17 s into the sequence, out of a total of 35 s (Video 1). In this animation, the transverse serial sections start at the base of the cone, move through the entire cone, and end at the cone's apex (Video 1). In the animation of longitudinal serial sections through the same cone, the video begins at one side of the cone and moves parallel to the long axis of the cone through the entire structure to end at the other side (Video 2).

Segmented 3D reconstructions—When the seed spirals in the recent *P. pinea* cone are segmented in 3D, the presence of three spirals is even more convincing. It also becomes visually evident that each row of seeds wraps around the cone in a spiral in a clockwise manner (Fig. 8D; Video 3). During the course of this study, over two dozen species of *Pinus* and of other genera in the Pinaceae, including at least one genus from each subfamily, have been scanned using microCT. All show three spirals of seeds, and the three spirals wrap around the cone several to multiple times, from cone base to apex, as in *P. pinea* (Fig. 8C, D; Video 3).

Once an internal tissue has been segmented—in this case, the seeds within the *P. pinea* cone—features of the Avizo software allow one to turn the object in three-dimensional space (e.g., Video 3). This makes it easy to determine the maximum number of seeds in one 360° revolution of the seed spiral as 17, for example (Table 1). It is also possible to measure internal structures, such as the length and width of the *P. pinea* seeds, for size analysis (Table 1).

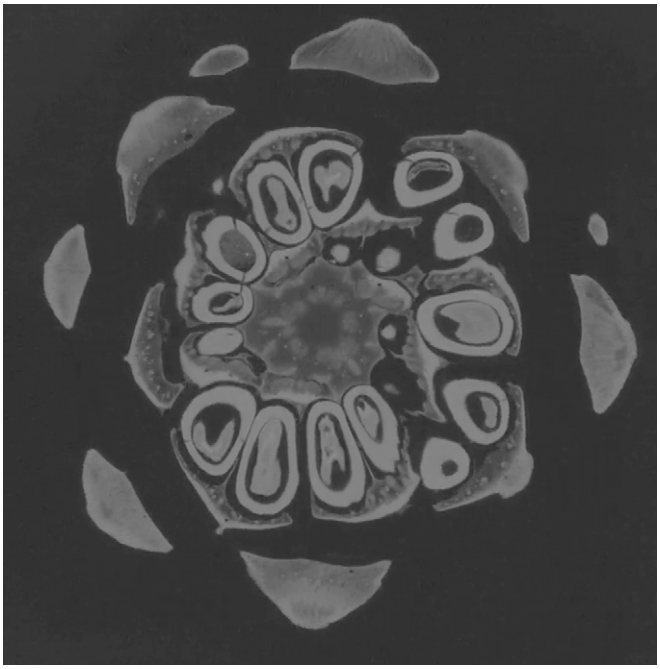

Video 1. Transverse serial sections through the seed cone of recent *Pinus pinea*, from the base of the cone to its apex, showing the presence of three spirals and their clockwise arrangement starting at ca. 17 s (out of a total of 35 s). This video is an MP4 file and can be viewed here with QuickTime or Windows Media Player, or can be viewed from the Botanical Society of America's YouTube channel.

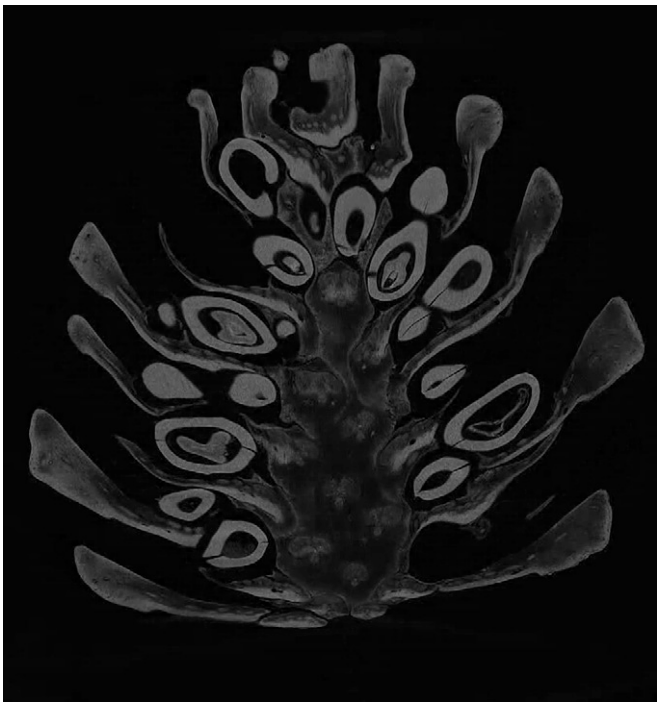

Video 2. Longitudinal serial sections through the same seed cone of recent *Pinus pinea* shown in Video 1. This video is an MP4 file and can be viewed here with QuickTime or Windows Media Player, or can be viewed from the Botanical Society of America's YouTube channel.

In fossil cones of morphotype 2, the body plan, in which three seed spirals wrap around the cone several times from base to tip, also becomes apparent when the seeds are segmented (Fig. 8F, H, I), which underlines the cones' affinity to the Pinaceae. In this morphotype, however, the chirality of the seed spirals differs from cone to cone; the seed spirals within a single cone can either

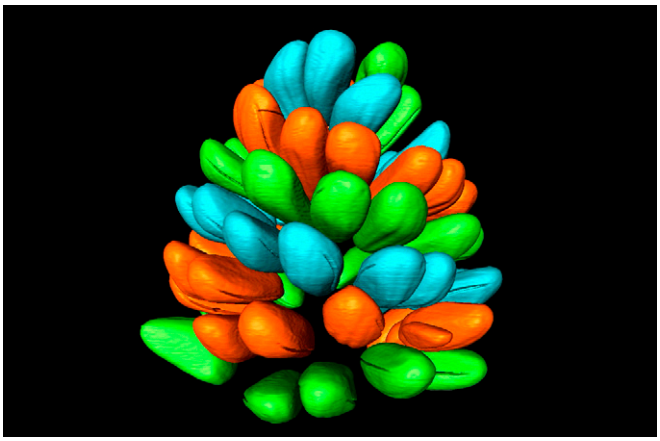

Video 3. Segmented seeds in a seed cone of recent *Pinus pinea*, showing their arrangement in three spirals that each wrap several times around the cone, from base to apex, in the same specimen shown in Videos 1 and 2. Segmentation by A. Schmitt. This video is an MPEG-1 file and can be viewed here with QuickTime or Windows Media Player, or can be viewed from the Botanical Society of America's YouTube channel.

TABLE 1. Comparison of the number of seed spirals, direction of seed spirals, number of seeds within one 360° revolution of the seed spiral, average seed length and width, and length to width ratio in one recent cone of *Pinus* and three fossil cones of putative pinaceous affinity.

Seed cone	No. of seed spirals	Direction of seed spiral	Maximum no. of seeds per 360° turn	Average seed length, mm	Average seed width at widest point, mm	Length : width ratio of seeds
Pinus pinea	3	Clockwise	17	18.1	9.1	2.0
Morphotype 2, spec. no. CG016	3	Clockwise	16	3.4	1.4	2.4
Morphotype 2, spec. no. CG061	3	Counterclockwise	16	3.6	1.7	2.1
Morphotype 2, spec. no. CG064	3	Counterclockwise	16	3.4	1.6	2.1

be arranged clockwise (Fig. 8E, F) or counterclockwise (Fig. 8G, H, I). Again, using the ability to manipulate the images in three-dimensional space with Avizo, a constant number of seeds per spiral (16) in this cone morphotype was counted in all three fossil examples (Table 1). The seeds in these fossil cones are similar in length and width, and have a ratio of seed length to seed width comparable to that in *P. pinea* (Table 1).

Integrated data from microCT sections and segmented 3D images— The phyllotaxy of seeds and cone scales in the Araucariaceae is quite different than in the Pinaceae in that araucarian cones have a different body plan altogether. MicroCT scanning and segmentation of eight cones of *Araucaria*—seven fossil cones and one recent cone—provides a reasonable sample set to begin looking at seed cone construction in araucarians.

Unlike the constant three seed spirals in Pinaceae cones, the number of seed spirals in *Araucaria* cones (e.g., Fig. 9A, D, G) is variable. In the eight *Araucaria* cones scanned, this varies from eight to 21 (Table 2). There is a general trend for larger cones to have a greater number of seed spirals, but there is no definite correlation between size as represented by circumference and the number of seed spirals (Table 2). For example, the recent cone of *A. araucana* (Molina) K. Koch with 20 seed spirals (Fig. 9G) has fewer seed spirals than a fossil cone of *A. mirabilis* (Speg.) Calder (Fig. 9D), which has 21, although the *A. araucana* cone is roughly 15 times larger in total volume.

In all *Araucaria* cones studied so far, the seed spirals begin at the base of the cone and end at the apex of the cone. In contrast to the Pinaceae, the seed spiral in an araucarian cone does not wrap around the cone multiple times. In fact, not all of the seed spirals even make a complete, 360° revolution around the cone. For example, in the case of the fossil *Araucaria* sp. cone from Wyoming (Fig. 9A), it was found that a seed spiral makes a 360° turn around the cone, from base to apex. In fact, the seed spiral extends slightly beyond 360° by about the width of two to three seeds. This becomes quite evident when the seeds, or in this instance the seed locules, which were used when it was not possible to mark the actual seeds, are segmented (Fig. 9B, C).

In the one other fossil cone of *Araucaria* illustrated here, *A. mirabilis* (Fig. 9D), the seed spiral makes only a half (180°) turn (Fig. 9E, F). In this cone, it is the actual seeds that have been segmented. The recent cone of *Araucaria*, *A. araucana* (Fig. 9G), which was scanned by microCT and partially segmented specifically for this comparison, shows that the row of seeds selected does not wrap around the cone in a spiral at all, but that the seeds are aligned one above another, from base to apex (Fig. 9H, I).

While clearest in the segmented 3D reconstructions, the extent of a seed spiral—whether forming a turn of 180°, 360°, or no turn at all—can also be interpreted from the length and curvature of the seed spirals in the 2D microCT sections, i.e., the greater the curvature, the greater the extent of the seed spiral around the cone. In the fossil *Araucaria* sp. cone from Wyoming (Fig. 9A), for example, the general length and curvature of the seed spirals are the greatest among these three cones of *Araucaria*, and thus supports the observation that the seed spirals in this cone make the greatest number of turns (one complete turn of 360°; Fig. 9B, C) among the three examples presented here. The general curvature of the seed spirals of *A. mirabilis* (Fig. 9D) is intermediate, accounting for its intermediate extent of a half-turn around the cone (180°; Fig. 9E, F). The generally straight-line rows of seed locules in the recent cone of *A. araucana* in 2D section (Fig. 9G) confirm that the seed locules, and hence seeds if the cone had been completely fertile, are aligned one above the another, from base to apex, making no turn at all around the cone (Fig. 9H, I).

DISCUSSION

The application of integrated microCT and scientific visualization with 3D segmentation within the framework of a study on 150-million-year-old conifer seed cones from the Late Jurassic of North America has made it possible to study the internal construction of these hard, dense, fossilized plant organs without specimen loss or damage, in high resolution on the micrometer scale, and with accurate detail. It was possible to observe diagnostic characters such as the number of seeds per cone scale, construction of the cone axis and vascular system, and phyllotaxy of the seeds and cone scales in monochromatic, single or serial 2D sections. Structures within the fossil cones were then reconstructed in three-dimensional space, and targeted tissues were segmented based on grayscale values with specific colors to make the internal structures more three-dimensionally expressive and thus graphically intuitive to the viewer.

In particular, the ease and rapidness of using microCT to produce transverse and longitudinal 2D sections of silicified plant organs, coupled with its nondestructiveness, makes it a powerful tool in paleobotany. Scanning with microCT is ideal for fossil specimens that are rare, unusual, or difficult to prepare. A comparison of the advantages and disadvantages of microCT with the conventional and still widespread method of thin-sectioning shows a great savings in time and labor in favor of microCT (Table 3). Nevertheless, thin-sections of silicified material have the occasional advantage of natural coloration in the plant tissues, as well as better resolution that may extend to the cellular level (Table 3). Thin-sections or cut, polished sections may also end up being the only option if internal tissues cannot be differentiated by microCT.

In the case of cone morphotype 2 from the Late Jurassic Morrison Formation, a still unnamed and undescribed conifer

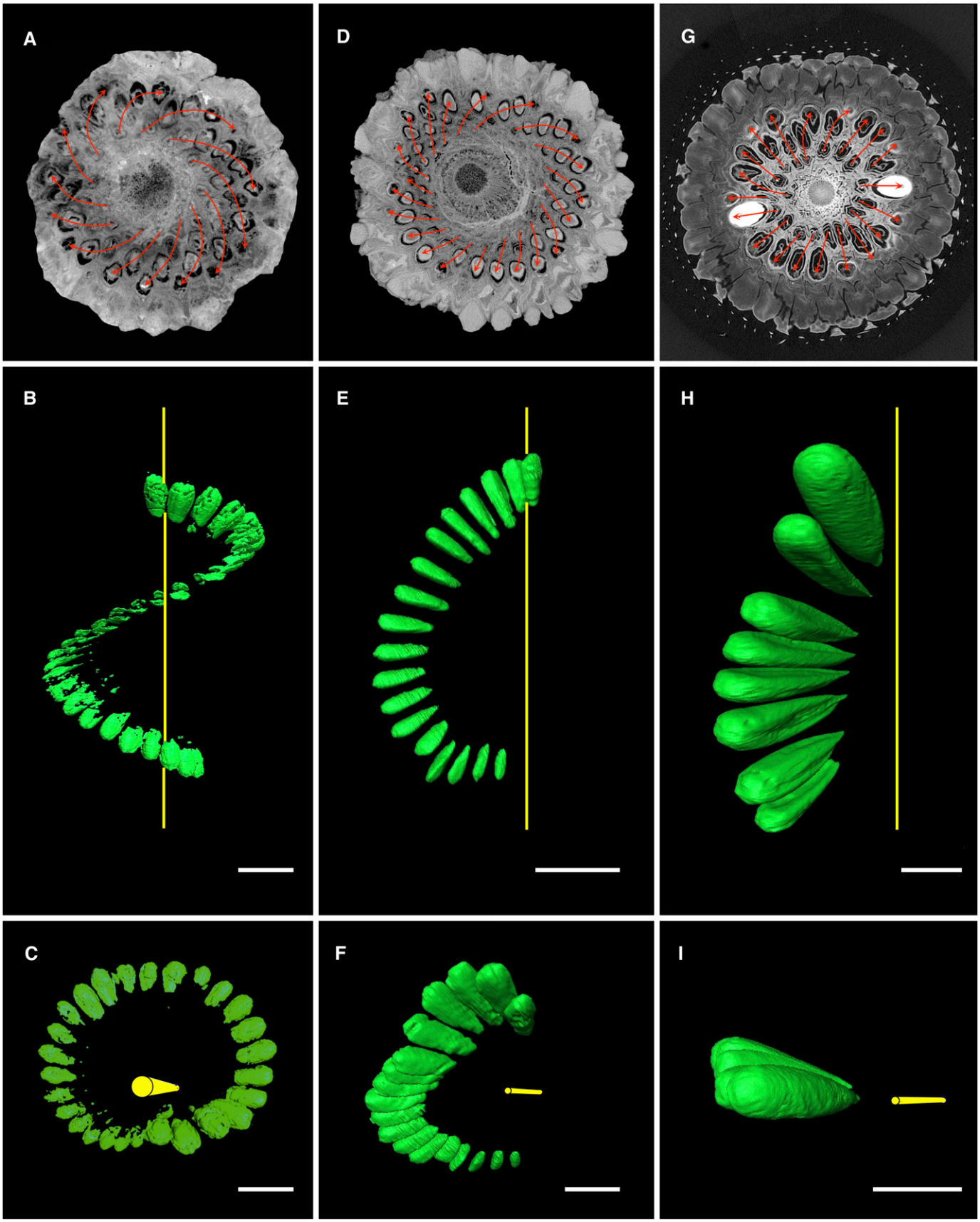

TABLE 2. Comparison of size and number of seed spirals in seven fossil cones and one recent cone of *Araucaria*.

Species	Geological age	Place of origin	Circumference at widest point, cm	No. of seed spirals	Source of cone, specimen number
A. araucana	Recent	Chile to western Argentina	53	20	Economic Botany Garden, University of Bonn, Nov. 2012
A. mirabilis	Middle Jurassic	Argentina	23.5	21	Museum für Naturkunde Chemnitz, K5640
A. mirabilis	Middle Jurassic	Argentina	20	13	Museum für Naturkunde Chemnitz, K5652
A. mirabilis	Middle Jurassic	Argentina	18.5	16	Museum für Naturkunde Chemnitz, K5679
A. mirabilis	Middle Jurassic	Argentina	16	8	Museum für Naturkunde Chemnitz, K5695
A. mirabilis	Middle Jurassic	Argentina	15.5	13	Museum für Naturkunde Chemnitz, K5694
A. mirabilis	Middle Jurassic	Argentina	12	13	Museum für Naturkunde Chemnitz, K5692
Araucaria sp.	Unknown, probably Mesozoic	Wyoming	19	21	Collection of Michael Flynn, Sheridan, WY, USA, CG066

seed cone from Utah, microCT coupled with 3D reconstruction and segmentation showed that the fossil cones bear two seeds per cone scale and a constant number of three spirals of seeds. If this species proves to pertain to the Pinaceae based on the cone scale–bract arrangement and phyllotaxy of its seeds, which can be clearly documented by microCT and 3D segmentation, this taxon will represent one of the oldest seed cones of this family in the fossil record (cf. *Eathiestrobus* G. W. Rothwell, Mapes, Stockey & J. Hilton [Rothwell et al., 2012], of comparable Late Jurassic age).

While having three seed spirals that revolve around the cone multiple times appears to be characteristic of the Pinaceae, as observed by microCT in numerous cones of recent species in this family, it appears that araucarian cones pursue a different strategy to achieve the optimal packing of seeds and cone scales within a spiral. For instance, an araucarian cone may compensate for a relatively lower number of seed spirals by extending the length of the seed spiral around the cone. As demonstrated here by 3D segmentation, the number of degrees in which a seed spiral wraps around the cone in different species of *Araucaria* can range from 0° to 180° to 360°, which was observed in *A. araucana*, *A. mirabilis*, and *Araucaria* sp. from Wyoming, respectively.

However, the seed spirals in cones of *Araucaria* spp. can even extend beyond a full revolution (>360°) around the cone. For example, it has been reported in the literature that the seed spirals in a cone of recent *A. angustifolia* (Bertol.) Kuntze (= *A. brasiliana* A. Rich.; Farjon, 1998), which is native to southern Brazil, wraps around the cone more than 1.5 times (Burlingame, 1914), forming a 540° turn around the cone. Furthermore, ongoing segmentation of additional fossil cones of *A. mirabilis* within the framework of the current study reveals that the seed spirals within a single cone can even wrap around the cone twice, thus forming two full turns around the cone equaling 720° (Weiser et al., 2013).

At this time, it is still unclear what exactly determines the number of times a seed spiral revolves around an araucarian cone—if it is contingent on taxonomy, the size or shape of the cone, factors related to the ontogenetic development of individual cones, or other factors. However, it is clear from the examples illustrated here that the organization of Araucariaceae seed cones fundamentally differs from those of the Pinaceae in regard to their phyllotaxy.

Serendipitously, the natural shape of most conifer seed cones makes them optimal for microCT scanning. The ideal shape for X-ray tomography is a cylinder because of the evenness of penetration of the X-rays into the object and the lack of edges (University of Texas at Austin, Department of Geological Sciences, 2013). Differential density preservation between tissues is necessary for good differentiation between internal tissues in fossil specimens. From my ongoing investigation of fossil plant material, it turns out that surprisingly good results can be obtained with silicified plant organs, despite the high density of their preservation with SiO_2. MicroCT on fossil conifer cones that were preserved in other ways, such as flattened carbonaceous compressions, three-dimensional coalified fossils, or external casts of plant organs, was found to be less successful in the current study. However, more comprehensive experience should be gained before the use of microCT for these preservational types can be completely ruled out. The experimental application of microCT for a wide range of plant fossils is currently underway by a number of research groups (see below).

Another X-ray technique, synchrotron radiation X-ray tomographic microscopy (SRXTM), is also proving to be extremely

←

Fig. 9 (see p. 10). Fossil and recent araucarian cones sectioned in 2D by microCT (A, D, G), and showing one segmented spiral or row of seeds or seed locules produced by 3D imaging (B, C, E, F, H, I). The seed spirals or rows in A, D, and G are delineated by red arrows. Yellow lines in B, C, E, F, H, and I represent the polar axis through the cones. Scale bars = 1 cm. (A–C) Fossil cone of *Araucaria* sp. from Wyoming (specimen no. CG066, Flynn Collection). (A) Transverse section 294/1012; diameter = ca. 6 cm. (B) Lateral view showing the 360° revolution of a single seed spiral. (C) Oblique distal view. (D–F) Fossil cone of *Araucaria mirabilis* from the Middle Jurassic of Argentina (specimen no. K5640, Museum für Naturkunde Chemnitz collection). (D) Transverse section 280/933; diameter = ca. 7.5 cm. (E) Lateral view showing the 180° revolution of a single seed spiral. (F) Oblique distal view. (G–I) Recent cone of *Araucaria araucana* from the Economic Botany Garden, University of Bonn, Germany. (G) Transverse section 469/876; diameter = ca. 17 cm. (H) Lateral view showing the vertical (nonspiral) arrangement of a row of seeds. (I) Oblique distal view.

TABLE 3. Comparison of the advantages and disadvantages of microCT with conventional thin-sectioning of fossil plant organs.

Point of comparison	MicroCT	Thin-sectioning
Destructive vs. nondestructive sampling	Nondestructive	Destructive
Time expenditure	Extremely rapid (ca. 1.5 h for specimen mounting, microCT scanning, and editing of files)	Time and labor consuming, extending over weeks or months
Color state	All internal structures monochromatic until color-coded by researcher	Tissues may be different in color due to different mineralogy or preservational histories.
Resolution quality	Good resolution on the tissue level, but not as good on the cellular level	Resolution may be better on the cellular and subcellular level.
Planes of sections	Both transverse and longitudinal planes of sections are easily produced by 3D visualization software	Can only cut cones in one plane of the section (transverse or longitudinal); or cone must be divided into sections for cutting in the different planes of the section.
Transfer of information from sections into 3D visualization software	Data are produced by microCT in electronic form that is readily transferred into 3D visualization software.	Thin-sections still need to be photographed, and those digital images registered (perfectly lined up in regard to one another), before transfer into 3D visualization software.
Operator	Easy operation of microCT and low time investment for scanning means that the researcher can perform preparation and scanning him- or herself, thereby increasing the likelihood that the desired results are obtained.	Due to the great amount of time and labor involved, the cutting, grinding, and polishing of thin-sections is usually done by a preparator or student, and continuous consultation is needed between researcher and laboratory worker.
Cost of set-up, maintenance, and supplies	Initial set-up costs, including microCT with dedicated computers and integrated tomographic software. Also, regular maintenance of the equipment and archiving of large data files.	Set-up cost of rock saws, grinding powder in various particle sizes, epoxy resins for attaching the sections to the slides, glass slides and cover slips. Also, compound microscope with digital photographic capabilities.

effective in elucidating the internal structure in some fossil plants (cf. Smith et al., 2009; Collinson et al., 2012a, b). SRXTM commonly offers finer resolution on the cellular level (cf. Friis et al., 2013a), unlike microCT which is optimal on the tissue level. The quality of results using SRXTM or microCT on the same specimens of Eocene fruits and seeds from Messel, Germany, was recently compared by Collinson et al. (2012b). A review paper on the application of SRXTM in the paleobotany of Cretaceous angiosperms is forthcoming (Friis et al., in press).

The first X-ray computed tomographic (CT) scanners were developed in the 1970s for use in human medicine, namely, as computed axial tomographic scanners (formerly known as CAT scanners). Since the early 1980s, these medical CT scanners had been used for nonmedical research such as that on large vertebrate fossils (Sutton, 2008, and references therein), on smaller objects such as dinosaur eggs (e.g., Mueller-Töwe et al., 2002), and even on a complex burrow system with a rodent nut cache encased in blocks of unconsolidated Miocene sand (Gee et al., 2003). At roughly the same time in the early 1980s, high-resolution X-ray computed tomography (microCT) for either medical or industrial applications, with voxel sizes ranging from 1 to 50 μm, was developed as well (see Pika-Biolzi et al., 2000, and references therein; Ritman, 2011).

The first exploratory study using microCT on fossil plants was carried out by Pika-Biolzi et al. (2000) on a trunk of the bennettitalean *Cycadeoidea* and on *A. mirabilis* cones. It was shown that high-resolution industrial CT could be used to discern internal tissues in these silicified plant parts, although thin-sections provided better resolution on the cellular level (Pika-Biolzi et al., 2000). Nevertheless, it was noted three years later that the application of microCT in botanical and paleobotanical research still lagged considerably behind its use in medical, geological, paleozoological, and zoological studies (Stuppy et al., 2003; see also Tafforeau et al., 2006). Even today, most microCT applications are biological, and they even include the scanning of live, intact animals (Ritman, 2011).

Recent technological progress has resulted in the development of relatively small microCT scanners, and the acquisition, use, and upkeep of a microCT scanner with integrated three-dimensional imaging software is within the budgetary and logistical reach of most moderately sized research institutions (e.g., Ritman, 2011; Abel et al., 2012). In particular, microCT scanners such as the phoenix v|tome|x s (General Electric Measurement & Control Solutions) used in the current study, as well as even smaller, "desktop" microCT scanners, are becoming more popular in the biological and paleontological sciences because of their compact size, low purchase price, and ease of operation (Ritman, 2011; Abel et al., 2012).

In the past decade, microCT—whether produced by a synchrotron radiation source or an industrial CT (nonmedical CT)—has been applied to types of fossil plant preservation other than the silicified cones described in the current study, such as pyritized Eocene fruits and seeds in silicone conservation fluid (DeVore et al., 2006), charcoalified seed fern pollen organs and ovules (Scott et al., 2009), organic-rich Eocene fruits and seeds that were flattened and embedded in an oil shale (Collinson et al., 2012a, b), and termite-bored Cretaceous silicified wood (Boucher, 2012), to name just a few examples.

In 2012, in a symposium at an international paleobotanical conference in Tokyo on the application of digital visualization methods to advance paleobotanical studies, eight talks described the use of various tomographic methods on fossil plants (Boucher, 2012; Collinson et al., 2012a; Friis et al., 2012; Gee et al., 2012; Murata et al., 2012; Nishida and Kotake, 2012; Smith et al., 2012; Wickens et al., 2012), which illustrates the current close embrace of paleobotany and tomography.

A survey of paleobotanical research incorporating X-ray tomographic microscopy shows that the number of studies has been on the increase since 2009 (Table 4). Most studies have been carried out on Cretaceous floral remains using SRXTM to produce

TABLE 4. General trends in the application of high-resolution X-ray computed tomography (microCT and SRXTM) and virtual scientific visualization in paleobotany.

Published study[a]	Paleobotanical material	Destructive sampling	Nondestructive sampling	Virtual 2D sectioning (orthoslices)	Virtual 3D surface reconstruction[b]	Virtual 3D cut-away or semitransparent images, or thin voltex slices[b]	Virtual 3D image segmentation	Computer animation
Pika-Biolzi et al., 2000	Jurassic bennettitalean trunk, Jurassic cone		MicroCT	X				
Gee et al., 2003	Miocene rodent food cache with nuts		Medical CT	X				
DeVore et al., 2006	Eocene fruit		MicroCT	X		Cut-away		
Friis et al., 2007	Cretaceous seed		PCXTM[c]	X	X			
Smith and Stockey, 2007	Eocene inflorescence	X					X	
von Balthazar et al., 2007	Cretaceous flower, pollen		SRXTM	X			X	
von Balthazar et al., 2008	Cretaceous flower		SRXTM	X				
Friis et al., 2009a	Cretaceous seeds		SRXTM	X	X			
Friis et al., 2009b	Cretaceous flower		SRXTM	X		Semitransparent	X	
Scott et al., 2009	Carboniferous seed fern reproductive organs		SRXTM	X	X			X
Smith et al., 2009	Recent fruits, seeds[d]		SRXTM	X	X		X	
Seyfullah et al., 2010	Permian seed fern ovule	X		X	X			
Friis and Pedersen, 2011	Cretaceous floral structures		SRXTM	X		Voltex		
Heřmanová et al., 2011	Cretaceous inflorescence		SRXTM	X				
Slater et al., 2011	Permian megaspores		SRXTM	X	X	Semitransparent		
von Balthazar et al., 2011	Cretaceous flowers		SRXTM	X		Semitransparent	X	
Friis and Pedersen, 2012	Cretaceous flower		SRXTM	X	X	Semitransparent; voltex		
Futey et al., 2012	Paleocene fruits		MicroCT	X				
Huang et al., 2012	Pliocene fruit		SRXTM	X				
Schönenberger et al., 2012	Cretaceous flower		SRXTM	X	X	Cut-away; semitransparent; voltex[f]		X
Friis et al., 2013a	Cretaceous flowers		SRXTM	X	X	Voltex		
Friis et al., 2013b	Cretaceous seeds		SRXTM, PCXTM[c]	X		Voltex		
Spencer et al., 2013	Carboniferous ovule		MicroCT[e]	X			X	
This study	Jurassic and nonfossil conifer cones		MicroCT	X			X	X

[a] Published abstracts of oral presentations not included.
[b] A type of volume rendering; no segmentation.
[c] Phase-contrast X-ray tomographic microscopy (cf. Tafforeau et al., 2006).
[d] Modern analogs for comparison with fossil material.
[e] MicroCT used to orient fossil for thin-sectioning.
[f] All three techniques used to create computer animations as well (M. Takahashi, personal communication).

2D sections. While it goes without saying that the form of scientific visualization selected for publication is determined by the nature of the material under study, objectives of the study, quality of results, and resources open to the researcher, an increasing number of studies are exploring other types of integrated visualization techniques such as 3D surface reconstructions, 3D cutaway, semitransparent or voltex (volume texture) reconstructions, 3D segmented reconstructions, or computer animations to gain further insight from their fossil material. In one particularly creative application, microCT was instrumental in visually locating a fossil ovule in the rock matrix to optimally position the fossil for destructive sampling by thin-sectioning (Spencer et al., 2013).

In general, a big step forward in the development of X-ray tomographic microscopy and visualization has been the integration of microCT with 3D image segmentation in paleontology. This has become routine in research fields such as vertebrate paleontology and includes the segmentation of brain cases in large dinosaurs (e.g., Rogers, 1998; Brochu, 2002; Witmer et al., 2008; Witmer and Ridgely, 2009), growth marks in the long bones of a fossil amphibian (e.g., Konietzko-Meier and Schmitt, 2013), the minute inner-ear structure in rare Jurassic mammals (Luo et al., 2011; Ruf et al., 2013), and the virtual preparation of fossils still embedded in a rock matrix (recent summary by Abel et al., 2012).

The same sort of close integration of microCT and 3D image segmentation has been slower to take off in paleobotany (Table 4; see also Kelber, 2013, "Links for Palaeobotanists" for a bibliographic overview). Only a handful of studies have employed 3D image segmentation on either recent (Smith et al., 2009) or fossil plants (Smith and Stockey, 2007; von Balthazar et al., 2007; Friis et al., 2009b; Smith et al., 2009; Spencer et al., 2013; current study). At the Tokyo symposium mentioned above, two of the eight talks described the integrated use of microCT with 3D segmented reconstructions (Gee et al., 2012; Murata et al., 2012).

Furthermore, the revolution in digital publishing and the widespread presence of online journals, which have gone from novel to normal in just over a decade, have also benefited this technology by making it possible to publish multimedia files such as videos or computer animations of scientific results produced by microCT (e.g., Scott et al., 2009; Schönenberger et al., 2012; Staedler et al., 2013, on recent plants). Examples include the computer animations published here (Videos 1–3), which show the internal construction in a recent *Pinus pinea* cone and the existence of three seed spirals in transverse serial section. The publication of computer animations was not possible before with print-only journals.

In summary, technologies and techniques arising from the digital revolution can be applied to gain new insights in long-established fields of botany such as plant morphology and paleobotany, as well as to transform these insights and results into more graphically expressive and intuitive visualizations of botanical structure and organization.

CONCLUSIONS

Within the framework of a larger study on fossil seed cones, microCT coupled with scientific visualization, 3D image segmention, and computer animation proved to be extremely effective in the nondestructive elucidation of internal structures and features, such as number of seeds per cone scale, and phyllotaxy of the seeds and cone scales. When applied to seed cones of living conifers, these techniques also reveal characters in the cone body plan that are useful for taxonomy. Compared to thin-sectioning, which is still the conventional technique used to prepare silicified fossil plants for study, microCT integrated with scientific visualization and 3D segmentation is faster, less laborious, and, most importantly, does not damage the specimens in the least, making it ideal for use on rare or precious fossil specimens. The current study on 150-million-year-old fossil plants from the Morrison Formation is the first publication describing the application of microCT integrated with virtual 2D serial sectioning, 3D image segmentation, and computer animation to silicified conifer cones.

LITERATURE CITED

Abel, R. L., C. R. Laurini, and M. Richter. 2012. A palaeobiologist's guide to 'virtual' micro-CT preparation. *Palaeontologia Electronica* 15(2): 15.2.6T.

Boucher, L. D. 2012. Three-dimensional modeling of termite galleries in Cretaceous silicified wood. *Japanese Journal of Palynology* 58: 22.

Brochu, C. A. 2002. Osteology of *Tyrannosaurus rex*: Insights from a nearly complete skeleton and high-resolution computed tomographic analysis of the skull. *Journal of Vertebrate Paleontology* 22(Supplement 4): 1–138.

Burlingame, L. L. 1914. The morphology of *Araucaria brasiliensis*. II. The ovulate cone and female gametophyte. *Botanical Gazette (Chicago, Ill.)* 57: 490–508.

Chandler, M. E. J. 1966. Fruiting organs from the Morrison Formation of Utah, U.S.A. *Bulletin of the British Museum (Natural History), Geology* 12: 137–171, plus 12 plates.

Collinson, M. E., S. Y. Smith, S. R. Manchester, V. Wilde, L. E. Howard, B. Robson, D. S. F. Ford, et al. 2012a. Digital visualization of fossil fruits and seeds from the Eocene Messel oil shale. *Japanese Journal of Palynology* 58: 35.

Collinson, M. E., S. Y. Smith, S. R. Manchester, V. Wilde, L. E. Howard, B. E. Robson, D. S. F. Ford, et al. 2012b. The value of X-ray approaches in the study of the Messel fruit and seed flora. *Palaeobiodiversity and Palaeoenvironments* 92: 403–416.

Daniels, F. J., and R. D. Dayvault. 2006. Ancient forests: A closer look at fossil wood. Western Colorado Publishing Company, Grand Junction, Colorado, USA.

Dayvault, R. D., and S. H. Hatch. 2007. Conifer cones from the Jurassic and Cretaceous rocks of eastern Utah. *Rocks and Minerals* 82: 382–396.

DeVore, M. L., P. Kenrick, K. B. Pigg, and R. A. Ketcham. 2006. Utility of high resolution X-ray computed tomography (HRXCT) for paleobotanical studies: An example using London Clay fruits and seeds. *American Journal of Botany* 93: 1848–1851.

Farjon, A. 1998. World checklist and bibliography of conifers. Royal Botanical Gardens, Kew, Richmond, Surrey, United Kingdom.

Friis, E. M., P. R. Crane, K. R. Pedersen, S. Bengtson, P. C. Donoghue, G. W. Grimm, and M. Stampanoni. 2007. Phase-contrast X-ray microtomography links Cretaceous seeds with Gnetales and Bennettitales. *Nature* 450: 549–552.

Friis, E. M., K. R. Pedersen, and P. R. Crane. 2009a. Early Cretaceous mesofossils from Portugal and eastern North America related to the Bennettitales-Erdtmanithecales-Gnetales Group. *American Journal of Botany* 96: 252–283.

Friis, E. M., K. R. Pedersen, M. von Balthazar, G. W. Grimm, and P. R. Crane. 2009b. *Monetianthus mirus* gen. et sp. nov., a nymphaealean flower from the Early Cretaceous of Portugal. *International Journal of Plant Sciences* 170: 1086–1101.

Friis, E. M., P. R. Crane, and K. R. Pedersen. 2011. Early flowers and angiosperm evolution. Cambridge University Press, Cambridge, United Kingdom.

Friis, E. M., and K. R. Pedersen. 2011. *Canrightia resinifera* gen. et sp. nov., a new extinct angiosperm with *Retimonocolpites*-type pollen

from the Early Cretaceous of Portugal: Missing link in the eumagnoliid tree? *Grana* 50: 3–29.

Friis, E. M., and K. R. Pedersen. 2012. *Bertilanthus scanicus*, a new asterid flower from the Late Cretaceous (late Santonian-early Campanian) of Scania, Sweden. *International Journal of Plant Sciences* 173: 318–330.

Friis, E. M., K. R. Pedersen, and P. K. Endress. 2012. Returning to old friends: Reexamination of *Silvianthemum suecicum* using SXRTM. *Japanese Journal of Palynology* 58: 62.

Friis, E. M., K. R. Pedersen, and P. K. Endress. 2013a. Floral structure of extant *Quintinia* (Paracryphiales, campanulids) compared with the Late Cretaceous *Silvianthemum* and *Bertilanthus. International Journal of Plant Sciences* 174: 647–664.

Friis, E. M., K. R. Pedersen, and P. R. Crane. 2013b. New diversity among chlamydospermous seeds from the Early Cretaceous of Portugal and North America. *International Journal of Plant Sciences* 174: 530–558.

Friis, E. M., F. Marone, K. R. Pederson, P. R. Crane, and M. Stampanoni. In press. Three-dimensional visualization of fossil flowers, fruits, seeds and other plant remains using synchrotron radiation x-ray tomographic microscopy (SRXTM): New insights into Cretaceous plant diversity. *Journal of Paleontology*.

Futey, M. K., M. A. Gandolfo, M. C. Zamaloa, R. Cúneo, and G. Cladera. 2012. Arecaceae fossil fruits from the Paleocene of Patagonia, Argentina. *Botanical Review* 78: 205–234.

Gee, C. T., P. M. Sander, and B. E. M. Petzelberger. 2003. A Miocene rodent nut cache in coastal dunes of the Lower Rhine Embayment, Germany. *Palaeontology* 46: 1133–1149.

Gee, C. T., and W. D. Tidwell. 2010. A mosaic of characters in a new whole-plant *Araucaria, A. delevoryasii* Gee sp. nov., from the Late Jurassic Morrison Formation of Wyoming, U.S.A. *In* C. T. Gee [ed.], Plants in Mesozoic time: Morphological innovations, phylogeny, ecosystems, 67–94. Indiana University Press, Bloomington, Indiana, USA.

Gee, C. T., A. Schmitt, and R. D. Dayvault. 2012. Micro CT and 3D analysis reveal complex internal structure in silicified conifer cones from the Late Jurassic Morrison Formation, USA. *Japanese Journal of Palynology* 58: 70.

General Electric Measurement and Control. 2013. vltomelx s. 2013. Website: http://www.ge-mcs.com/en/metrology/3d-metrology/vtomex-s.html [accessed 11 July 2013].

Harris, T. M. 1976. Two neglected aspects of fossil conifers. *American Journal of Botany* 63: 902–910.

Heřmanová, Z., J. Kvaček, and E. M. Friis. 2011. *Budvaricarpus serialis* Knobloch & Mai, an unusual new member of the Normapolles Complex from the Late Cretaceous of the Czech Republic. *International Journal of Plant Sciences* 172: 285–293.

Huang, Y., F. M. B. Jacques, Y.-S. Liu, T. Su, Y. Xing, X. Xiao, and Z. Zhou. 2012. New fossil endocarps of *Sambucus* (Adoxaceae) from the upper Pliocene in SW China. *Review of Palaeobotany and Palynology* 171: 152–163.

Kelber, K. P. 2013. Links for Palaeobotanists. Website http://www.equisetites.de/palbot/tools/microtomography.html [accessed 19 September 2013].

Konietzko-Meier, D., and A. Schmitt. 2013. *Plagiosuchus* femur histology and growth deduced from thin section in comparison to microCT-scanning. *Netherlands Journal of Geoscience — Geologie en Mijnbouw* 92: 97–108.

Kowallis, B. J., E. H. Christiansen, A. L. Deino, F. Peterson, C. E. Turner, M. J. Kunk, and J. D. Obradovich. 1998. The age of the Morrison Formation. *Modern Geology* 221: 235–260.

Luo, Z.-X., I. Ruf, J. A. Schultz, and T. Martin. 2011. Fossil evidence on evolution of inner ear cochlea in Jurassic mammals. *Proceedings of the Royal Society of London. Series B. Biological Sciences* 278: 28–34.

Mueller-Töwe, I. J., P. M. Sander, D. Thies, and H. Schüller. 2002. Hatching and infilling of dinosaur eggs as revealed by computed tomography. *Palaeontographica Abt. A* 267: 119–168.

Murata, A., H. Nishida, and T. A. Ohsawa. 2012. 3D reconstruction of a coleopteran pupa in a reproductive organ of an extinct gymnosperm from the Upper Cretaceous of Hokkaido, Japan. *Japanese Journal of Palynology* 58: 163.

Nishida, H., and Y. Kotake. 2012. 3D observation of fruit-like organs of two extinct gymnosperm groups from the Late Cretaceous of Hokkaido using MXCT. *Japanese Journal of Palynology* 58: 169.

Parrish, J. T., F. Peterson, and C. E. Turner. 2004. Jurassic "savannah"—Plant taphonomy and climate of the Morrison Formation (Upper Jurassic, Western USA). *Sedimentary Geology* 167: 137–162.

Peterson, F. Undated. Summary list of Late Jurassic plants, Western Interior U.S. & SW Canada. Website www.webpages.uidaho.edu/~jparrish/Morrison_plants.pdf [accessed 3 May 2013].

Pika-Biolzi, M., P. A. Hochuli, and A. Flisch. 2000. Industrial X-ray computed tomography applied to paleobotanical research. *Rivista Italiana di Paleontologia e Stratigrafia* 106: 369–378.

Ritman, E. L. 2011. Current status of developments and applications of microCT. *Annual Review of Biomedical Engineering* 13: 531–552.

Rogers, S. W. 1998. Exploring dinosaur neurobiology: Computed tomography scanning and analysis of an *Allosaurus fragilis* endocast. *Neuron* 21: 673–679.

Rothwell, G. W., G. Mapes, R. A. Stockey, and J. Hilton. 2012. The seed cone *Eathiestrobus* gen. nov.: Fossil evidence for a Jurassic origin of Pinaceae. *American Journal of Botany* 99: 708–720.

Ruf, I., Z.-X. Luo, and T. Martin. 2013. Reinvestigation of the basicranium of *Haldanodon exspectatus* (Mammaliaformes, Docodonta). *Journal of Vertebrate Paleontology* 33: 382–400.

Rutishauser, R., and P. Peisl. 2001. Phyllotaxy. *Wiley Online Library* [accessed 14 May 2013].

Schindelin, J., I. Arganda-Carreras, E. Frise, V. Kaynig, M. Longair, T. Pietzsch, S. Preibisch, et al. 2012. Fiji: An open-source platform for biological-image analysis. *Nature Methods* 9: 676–682.

Schönenberger, J., M. von Balthazar, M. Takahashi, X. Xiao, P. R. Crane, and P. S. Herendeen. 2012. *Glandulocalyx upatoiensis*, a fossil flower of Ericales (Actinidiaceae/Clethraceae) from the Late Cretaceous (Santonian) of Georgia, USA. *Annals of Botany* 109: 921–936. Supplementary data available at doi:10.1093/aob/mcs009.

Scott, A. C., J. Galtier, N. J. Gostling, S. Y. Smith, M. E. Collinson, M. Stampanoni, F. Marone, et al. 2009. Scanning electron microscopy and synchrotron radiation X-ray tomographic microscopy of 330 million year old charcoalified seed fern fertile organs. *Microscopy and Microanalysis* 15: 166–173.

Seyfullah, L. J., J. Hilton, M.-M. Liang, and S.-J. Wang. 2010. Resolving the systematic and phylogenetic position of isolated ovules: A case study on a new genus from the Permian of China. *Botanical Journal of the Linnean Society* 164: 84–108.

Slater, B. J., S. McLoughlin, and J. Hilton. 2011. Guadalupian (middle Permian) megaspores from a permineralised peat in the Bainmedart Coal Measures, Prince Charles Mountains, Antarctica. *Review of Palaeobotany and Palynology* 167: 140–155.

Smith, S. Y., and R. A. Stockey. 2007. Establishing a fossil record for the perianthless Piperales: *Saururus tuckerae* sp. nov. (Saururaceae) from the Middle Eocene Princeton Chert. *American Journal of Botany* 94: 1642–1657.

Smith, S. Y., M. E. Collinson, P. J. Rudall, D. A. Simpson, F. Marone, and M. Stampanoni. 2009. Virtual taphonomy using synchrotron tomographic microscopy reveals cryptic features and internal structure of modern and fossil plants. *Proceedings of the National Academy of Sciences, USA* 106: 12013–12018.

Smith, S. Y., J. C. Benedict, M. E. Collinson, J. Skornickova, V. Wilde, F. Marone, J. L. Fife, et al. 2012. Seed morphology and evolution in Zingiberales: Insights from SRXTM. *Japanese Journal of Palynology* 58: 218–219.

Spencer, A. R. T., J. Hilton, and M. D. Sutton. 2013. Combined methodologies for three-dimensional reconstruction of fossil plants preserved in siderite nodules: *Stephanospermum braidwoodensis* nov. sp. (Medullosales) from the Mazon Creek lagerstätte. *Review of Palaeobotany and Palynology* 188: 1–17.

Staedler, Y. M., D. Masson, and J. Schönenberger. 2013. Plant tissues in 3D via X-ray tomography: Simple contrasting methods allow high resolution imaging. *PLoS ONE* 8: e75295 .

Stuppy, W. H., J. A. Maisano, M. W. Colbert, P. J. Rudall, and T. B. Rowe. 2003. Three-dimensional analysis of plant structure using

high-resolution X-ray computer tomography. *Trends in Plant Science* 8: 2–6.

Sutton, M. D. 2008. Tomographic techniques for the study of exceptionally preserved fossils. *Proceedings of the Royal Society of London. Series B. Biological Sciences* 275: 1587–1593.

Tafforeau, P., R. Boistel, E. Boller, A. Bravin, M. Brunet, Y. Chaimanee, P. Cloetens, et al. 2006. Applications of X-ray synchrotron microtomography for non-destructive 3D studies of paleontological specimens. *Applied Physics. A, Materials Science & Processing* 83: 195–202.

Tidwell, W. D. 1990. Preliminary report on the megafossil flora of the Upper Jurassic Morrison Formation. *Hunteria* 2: 1–11.

University of Texas at Austin, Department of Geological Sciences. 2013. High resolution X-ray CT facility. Website http://www.ctlab.geo.utexas.edu/overview/ [accessed 10 May 2013].

von Balthazar, M., K. R. Pedersen, P. R. Crane, M. Stampanoni, and E. M. Friis. 2007. *Potomacanthus lobatus* gen. et sp. nov., a new flower of probable Lauraceae from the Early Cretaceous (early to middle Albian) of eastern North America. *American Journal of Botany* 94: 2041–2053.

von Balthazar, M., K. R. Pedersen, P. R. Crane, and E. M. Friis. 2008. *Carpestella lacunata* gen. et sp. nov., a new basal angiosperm flower from the Early Cretaceous (early to middle Albian) of eastern North America. *International Journal of Plant Sciences* 169: 890–898.

von Balthazar, M., P. R. Crane, K. R. Pedersen, and E. M. Friis. 2011. New flowers of Laurales from the Early Cretaceous (Early to Middle Albian) of eastern North America. *In* L. Wanntorp and L. P. Ronse de Craene [eds.], Flowers on the tree of life, 49–87. Cambridge University Press, Cambridge, United Kingdom.

Watson, J., H. K. Fisher, and N. Hall. 1987. A new species of *Brachyphyllum* from the English Wealden and its probable female cone. *Review of Palaeobotany and Palynology* 51: 169–187.

Weiser, K., A. Weigand, C. T. Gee, and R. Rössler. 2013. Phyllotaxy in seed cones of *Araucaria mirabilis* (Middle Jurassic Cerro Cuadrado Petrified Forest, Patagonia, Argentina)—Preliminary observations. *In* J. Reitner, Q. Yang, Y. Wang, and M. Reich [eds.], Palaeobiology and geobiology of fossil lagerstätten through earth history, 184–185. Universitätsdrucke Göttingen, Göttingen, Germany.

Wickens, Z. J., A. R. T. Spencer, J. Hilton, and M. D. Sutton. 2012. Tomography old and new: Comparison of 3D reconstruction techniques for fossil plants. *Japanese Journal of Palynology* 58: 257.

Witmer, L. M., and R. C. Ridgely. 2009. New insights into the brain, braincase, and ear region of tyrannosaurs (Dinosauria, Theropoda), with implications for sensory organization and behavior. *The Anatomical Record* 292: 1266–1296.

Witmer, L. M., R. C. Ridgely, D. L. Dufeau, and M. C. Semones. 2008. Using CT to peer into the past: 3D visualization of the brain and ear regions of birds, crocodiles, and non-avian dinosaurs. *In* H. Endo and R. Frey [eds.], Anatomical imaging: Towards a new morphology, pp. 67–88. Springer-Verlag, Tokyo, Japan.